Title
Photochemical internalization enhanced macrophage delivered chemotherapy

Authors
Shin, Diane
Christie, Catherine
Ju, David
et al.

Publication Date
2018-03-01

DOI
10.1016/j.pdpdt.2017.12.002

Peer reviewed

HHS Public Access

Author manuscript

Photodiagnosis Photodyn Ther. Author manuscript; available in PMC 2018 March 28.

Published in final edited form as:

Photodiagnosis Photodyn Ther. 2018 March ; 21: 156–162. doi:10.1016/j.pdpdt.2017.12.002.

Photochemical internalization enhanced macrophage delivered chemotherapy

Diane Shin[a,*], **Catherine Christie**[a,1], **David Ju**[a], **Rohit Kumar Nair**[a], **Stephanie Molina**[b], **Kristian Berg**[c], **Tatiana B. Krasieva**[a], **Steen J. Madsen**[b], and **Henry Hirschberg**[a]

[a]Beckman Laser Institute and Medical Clinic, University of California, Irvine 1002 Health Sciences Rd, Irvine, CA, 92617, United States

[b]Dept. of Health Physics and Diagnostic Sciences, University of Nevada, Las Vegas 4505 S. Maryland Pkwy, Las Vegas, NV, 89154-3037, United States

[c]Dept. of Radiation Biology, The Norwegian Radium Hospital, Oslo University Hospital, Montebello, N-0310, Oslo, Norway

Abstract

Background—Macrophage (Ma) vectorization of chemotherapeutic drugs has the advantage for cancer therapy in that it can actively target and maintain an elevated concentration of drugs at the tumor site, preventing their spread into healthy tissue. A potential drawback is the inability to deliver a sufficient number of drug-loaded Ma into the tumor, thus limiting the amount of active drug delivered. This study examined the ability of photochemical internalization (PCI) to enhance the efficacy of released drug by Ma transport.

Methods—Tumor spheroids consisting of either F98 rat glioma cells or F98 cells combined with a subpopulation of empty or doxorubicin (DOX)-loaded mouse Ma (RAW264.7) were used as in vitro tumor models. PCI was performed with the photosensitizer $AlPcS_{2a}$ and laser irradiation at 670 nm.

Results—RAW264.7 Ma pulsed with DOX released the majority of the incorporated DOX within two hours of incubation. PCI significantly increased the toxicity of DOX either as pure drug or derived from monolayers of DOX-loaded Ma. Significant growth inhibition of hybrid spheroids was also observed with PCI even at subpopulations of DOX-loaded Ma as low as 11% of the total initial hybrid spheroid cell number.

Conclusion—Results show that RAW264.7 Ma, pulsed with DOX, could effectively incorporate and release DOX. PCI significantly increased the ability of both free and Ma-released DOX to inhibit the growth of tumor spheroids in vitro. The growth of F98+DOX loaded Ma hybrid

[*]Corresponding author. diane.shin77@gmail.com (D. Shin).
[1]These have contributed equally to this work.

Conflict of interest

All of the authors declare that she/he has no conflict of interest.

Ethical approval

This article does not contain any studies with human participants or animals performed by any of the authors.

Compliance with Ethical Standards:

spheroids were synergistically reduced by PCI, compared to either photodynamic therapy or released DOX acting alone.

Keywords

Photochemical internalization; PCI; Macrophage drug delivery; Doxorubicin; Photodynamic therapy; PDT

1. Introduction

Current treatment for many cancers often start with surgical resection followed by various post-operative treatments such as chemotherapy and/or radiotherapy. The primary goal of post-operative treatment is to reduce or eliminate tumor recurrence due to remaining malignant cells residing in the margin of the resection cavity. Targeted delivery approaches of chemotherapeutic drugs, such as cell-based vectorization, may result in improved outcomes since they can target and maintain elevated drug concentrations at the tumor site and prevent their spread into healthy tissue [1,2]. In contrast to nanoparticles, cells such as monocytes, Ma, and stem cells migrate to and infiltrate into tumors via an active process, despite stromal barriers and the elevated interstitial pressure present in most tumors. Ma are attracted by chemotactic factors secreted by tumors, especially from hypoxic regions, where conventional chemo and radiation therapy are least effective [3,4]. Furthermore, Ma are highly resistant to many anticancer drugs in comparison to tumor cells [5]. Ma also have the important advantage in that they can be obtained from the patient by leukapheresis, loaded *ex vivo* with drugs and reinjected into the blood.

Previous studies have demonstrated the feasibility of delivering loaded nanoparticles or water-soluble drugs to tumors using Ma. These include transport of gold nanorods to target breast cancer cells [6], adenovirus to prostate tumors [7], gold nanoshells to gliomas or squamous cell carcinomas [8–10], DOX to lung metastasis from breast tumors [11] and drug-loaded nanoparticles to human breast tumors [12]. Although the experimental results obtained so far are promising, one important limitation is infiltration of a sufficient number of exogenous drug-loaded Ma into the tumor. This limits the concentration of active drug that can be delivered to the tumor microenvironment. Therefore, methods to enhance the efficacy of the Ma transported and released drug would offer a distinct therapeutic advantage.

PCI has previously been demonstrated to enhance the effects of a large number of macromolecules (including chemotherapeutic agents) that are subject to endosome-lysosome entrapment [13–16]. PCI is a technique, which utilizes the photochemical properties of photodynamic therapy (PDT), for the enhanced and site-specific delivery of drugs into the cell cytoplasm. Drugs that are internalized into cells via endocytosis end up trapped in intracellular endosomes and lysosomes. The concept of PCI is based on using photosensitizers, which localize in the cell membrane and are carried into the cell forming the endosome membrane. The photosensitizer remains in the endosome membrane while the macromolecule is localized within the lumen. Specific amphiphilic photosensitizers like disulfonated aluminum phthalocyanine ($AlPcS_{2a}$) or *meso*-tetraphenyl chlorin disulphonate

($TPCS_{2a}$), preferentially accumulate in the membranes of endosomes and lysosomes. Upon light exposure, the photosensitizer interacts with ambient oxygen to produce singlet oxygen, which ruptures the vesicular membrane. The released agent can therefore exert its full biological activity, in contrast to being degraded by lysosomal hydrolases following endosome-lysosome fusion.

The basic concept of drug loaded Ma-PCI is illustrated in Fig. 1. The aim of the present work was to evaluate the ability of $AlPcS_{2a}$ PCI to enhance the efficacy of DOX released from loaded Ma. Supernatants from DOX-loaded Ma were evaluated for their ability to inhibit the growth of multi-cell three dimensional glioma spheroids with and without PCI. In addition, PCI experiments were performed utilizing a subpopulation of DOX-loaded Ma incorporated into glioma hybrid spheroids, as a simulation of limited Ma penetration into tumors.

2. Materials and methods

2.1. Cell lines and drug

The murine macrophages RAW264.7 (designated Ma) and F98 rat glioma cells were obtained from the American Type Culture Collection (Manassas, VA). Both cell lines were maintained in Advanced DMEM medium (Thermo Fisher Scientific, Carlsbad, CA) supplemented with 2% heat-inactivated fetal bovine serum (FBS), 25mM HEPES buffer, 100 U/ml penicillin and 100 μg/ml streptomycin at 37 °C, 5% CO_2 and 95% humidity. The F98 and Ma cells were grown as monolayers in T-25 tissue culture flasks, Greiner BioOne (Frickenhausen Germany) and in 9 cm flat-bottomed square dishes (Simport Scientific Beloeil, QC, Canada) respectively. Doxorubicin Hydrochloride (DOX) was obtained from Sigma Aldrich (St. Louis, MO).

2.2. Ma DOX supernatant production

Ma cells were incubated in 9 cm square dishes until sub-confluent. The medium was replaced with medium containing DOX solution (100 μg/ml) for 2 min. The Ma were washed four times directly in the dishes to remove all non-incorporated drug and the cultures were incubated in fresh medium. Portions of the supernatants were harvested after 5 and 120 min. Supernatants were also harvested from monolayers of “empty” Ma (not pulsed with DOX), which acted as controls.

2.3. Toxicity of DOX on F98 and RAW264.7 Ma

To test the toxic effects of DOX directly on Ma or F98 cell monolayers, 5×10^3 of both cell types were aliquoted into the wells of flat bottomed tissue culture microplates. Monolayer cultures were used in these experiments since the Ma do not form spheroids. Twenty-four hours later, DOX was added to the wells at increasing concentrations and the incubation was continued for 96 h, at which point the culture medium was replaced with fresh clear buffer containing MTS reagent (MTS, Promega, Madison, WI) which was used to determine cell viability. Cells were incubated in MTS reagents for 2 h. The optical density was measured using an ELx800uv Universal Microplate Reader (Bio-Tek Instruments, Inc, Winooski, VT).

2.4. PCI enhanced toxicity of DOX or active supernatants on F98 spheroids

F98 spheroids were formed by a modification of the centrifugation method previously described [15]. F98 glioma spheroids were generated with 2.5×10^3 cells in 200 μl of culture medium per well of an ultra-low attachment surface 96-well round-bottomed plate (Corning Inc., NY). Immediately following centrifugation, the tumor cells formed into a disk shape. The plates were maintained at 37 °C in a 5% CO_2 incubator for 24 h to allow them to take on the usual three-dimensional spheroid form.

Twenty-four hours after spheroid generation, 0.5 μg/ml of the photosensitizer ($AlPcS_{2a}$, Frontier Scientific, Inc., Logan, UT) was added. Eighteen hours later the spheroids were washed four times. DOX as pure drug or active supernatant at increasing concentrations was added in fresh medium. Four hours after DOX or supernatant was added, light treatment, $\lambda = 670$ nm, from a diode laser (Intense, North Brunswick, NJ) at an irradiance of 2.0 mW/cm^2 was administered for 8.0 or 10 min, corresponding to radiant exposures of 0.96 or 1.2 J/cm^2 respectively.

Control cultures received light treatment but no DOX (PDT control) or DOX but no illumination (drug only control). Following PCI, the plates were returned to the incubator. Typically, 8–16 spheroids were followed for each group for up to 14 days of incubation. Culture medium in the wells was exchanged every third day. Determination of spheroid growth was carried out by averaging two measured perpendicular diameters of each spheroid using a microscope with a calibrated eyepiece micrometer and their volume calculated assuming a perfect sphere.

2.5. Assessment of PCI mediated incorporation of drug-loaded macrophage on spheroid growth

Sub-confluent F98 cells in T-25 flasks were incubated in 5 ml of medium containing 0.5 μg/ml of $AlPcS_{2a}$ for 18 h. The cells were washed three times in fresh medium, detached from the flask by enzyme treatment and counted.

Ma cells were incubated in 9 cm square dishes until sub-confluent. The Ma were treated with mitomycin C to prevent cell division and their subsequent contribution to spheroid growth. Twenty-four hours following mitomycin C treatment, the medium was replaced with medium containing DOX solution (100 μg/ml) for 5 min. The Ma were washed four times in the dish and then removed from the plastic by mechanical scraping and counted. DOX-loaded Ma are designated as Ma^{DOX}.

To form hybrid spheroids, Ma^{DOX} or “empty” Ma were mixed with F98 tumor cells at ratios of tumor cells to Ma or Ma^{DOX} ranging from 2:1 to 8:1 (33–11%). In all cases, 4×10^3 F98 cells and a variable number of Ma were aliquoted into each well of an ultra-low attachment surface 96-well round-bottomed plate. The plates were centrifuged at 1000*g* for 10 min as previously described. Four hours after spheroid generation, light treatment at an irradiance of 2.0 mW/cm^2 was administered for 10 min (1.2 J/cm^2). Control cultures received no Ma, empty Ma or Ma^{DOX} but no illumination. The hybrid spheroids were monitored for growth for an additional 14 days as previously described.

2.6. Statistical analysis

Microsoft Excel was used to determine the mean and standard deviation. Data were analyzed using one-way ANOVA at the significance level of $p < 0.05$ and presented as mean with standard deviation unless otherwise noted.

Two values were considered distinct when their *p*-values were below 0.05. In order to determine the degree of synergism between PDT, Ma^{DOX} and PCI-Ma^{DOX} the following equation was used (Eq. (1))

$$\alpha = \frac{SF^{PDT} \times SF^{DOX}}{SF^{PCI-MaDOX}} \quad (1)$$

The numerator includes the product of the surviving fraction (SF) of the individual treatments separately and the denominator includes the surviving fraction of the combined treatments. A value of $\alpha = 1$ indicates an additive effect. A value of $\alpha < 1$ or $\alpha > 1$ indicates an antagonistic or synergistic effect, respectively.

3. Results and discussion

3.1. Loading and release of DOX from Ma^{DOX} and F98

3×10^4 Ma or F98 cells were plated out in 35mm glass-bottomed imaging dishes (Fluorodish Cell Culture Dish, FL, USA) and incubated in culture medium for 24 h to allow them to adhere. The medium was replaced with fresh medium containing 100 μg/ml of DOX (Ma cells) or 10 μg/ml DOX (F98 cells). Ma and F98 cells were incubated in DOX medium for 2 and 30 min, respectively. The incubation was terminated by a double wash in clear buffer to remove non-incorporated DOX. Confocal microscopy was carried out after 15, 120 and 180 min in order to evaluate the time release of DOX from the two cell types. The ability of Ma cells (designated Ma^{DOX}) to incorporate and release soluble DOX is illustrated in Fig. 2a–c. At a 15 min incubation time point (Fig. 2a), DOX could be visualized mainly in the cell cytoplasm and around the nuclear membrane, with little drug in the nucleus. After 2 h of incubation (Fig. 2b) most of the drug was out of the Ma and by hour three, no DOX was detectable (Fig. 2c). The multi-drug resistant protein P-gp, which actively pumps drug molecules out of the cell, is highly expressed in the RAW264.7 Ma cell line used in the present study. This possibly could account for the relatively rapid export of drug from Ma. The incorporation of DOX in F98 glioma cells is shown in Fig. 2d–f). The cells were incubated with DOX (10 μg/ml for 30 min), and excess DOX was removed by multiple wash cycles. After fifteen minutes of incubation in fresh medium confocal microscopy could demonstrate DOX mainly on the nuclear and nucleolus membranes, in the cell cytoplasm but with little diffused DOX within the nucleus (Fig. 2d). This is more clearly demonstrated in Fig. 2e done at a greater magnification. The intracellular DOX distribution was similar to that previously demonstrated for the resistant human breast tumor cell line MCF-7/ADR and the human carcinoma cell line, Ca9-22 [17,18]. The drug concentration and distribution appears to be unchanged over the three-hour period studied, although a low concentration of DOX was now visible in the nucleus (Fig. 2f). Compared to F98 cells, Ma^{DOX} appeared to

release the drug much more rapidly, with most of the drug released in the first 3 h of incubation (Fig. 2c). These release results are in agreement with those of Fu et al. who showed that most of the DOX in the RAW264.7 Ma was released into the media during the first two hours of incubation, as determined by HPLC [11].

3.2. Effects of free DOX on F98 and Ma

Cell viability was tested using the MTS assay. As shown in Fig. 3a, F98 cells were much more sensitive to DOX compared to Ma, which appeared highly resistant to the drug. Ma in general have been demonstrated to be highly resistant to many anti-cancer drugs in comparison to tumor cells [5]. The effects of free DOX on spheroid growth are shown in Fig. 3b. Compared to F98 monolayer cultures, the spheroids were much more resistant to the toxic effects of the drug. This difference between 2D and 3D cell cultures has been established previously [19]. Tumor spheroids mimic *in vivo* tumors in their microenvironment and, as such, are superior to monolayer cultures for this type of in vitro study as they represent a bridge to in vivo animal experiments.

3.3. Inhibitory effects of PCI-DOX on F98 spheroids

The ability of PCI to enhance the toxicity of DOX as measured by the growth inhibition of F98 spheroids is shown in Fig. 4. Significant inhibition of PCI-treated spheroid growth, compared to drug alone, was seen for DOX concentrations of 0.05 and 0.1 μg/ml at both light fluence levels tested. The inhibitory effect was clearly synergistic for the two highest DOX levels examined at both fluences (0.96 and 1.2 J/cm^2). The α values calculated for these two DOX concentrations were 1.2 and 1.4 respectively for 0.96 J/cm^2, and 2.3 and 4.5 for a fluence level of 1.2 J/cm^2.

A synergistic response between the photosensitizer $AlPcS_{2a}$, PDT and free DOX has been shown in Ca9-22 cells in vitro regardless of whether the drug was added before or after PDT light treatment [18]. PCI DOX has also been shown capable of reversing DOX drug resistance in the doxorubicin resistant MCF-7/ADR cell lines [17]. Additionally, AlS_2Pc-mediated PDT has been shown to enhance the effects of DOX on mice bearing murine leukemia and lymphoma compared to chemotherapy alone [20]. In contrast to these results, the combination of PDT and DOX was only additive on DOX sensitive MCF-7 human breast cancer cells assayed by either MTT or colony inhibition assays [17,21]. Based on its water solubility and molecular weight (580 g/mol), one would expect the effects of DOX to be enhanced in a PCI protocol, as was observed with the F98 glioma cell line used in the present work. As seen in Fig. 2e and f, free DOX accumulated in cytosolic granules, indicating that the drug is trapped in *endo*-lysosome vesicles. However, as illustrated from the aforementioned studies, the synergy of PCI with DOX appears to be cell line dependent.

PCI has been proven effective employing light treatment protocols either before or after drug administration [22,23]. In the case of PCI with DOX, it appears that the light before sequence is more effective than the light after [17,18]. In the experiments reported here, free DOX was added to the cultures immediately after the wash cycle followed by a 4 h incubation period prior to initiation of light treatment. Since additional wash cycles were not used to remove any remaining DOX from the cultures, it is assumed that active drug was still

available post light treatment and therefore this protocol can be considered a combined light "after" and light "before" sequence. The pronounced synergistic effect of PCI DOX on F98 spheroids was likely due to a combination of both facilitating its *endo*-lysosomal release (light after sequence) and by preventing lysosomal uptake of DOX (light before sequence).

3.4. PCI of DOX released from loaded Ma

Similar spheroid experiments as those described above for PCI of free DOX were performed employing supernatants containing released DOX from DOX-loaded Ma. The Ma were pulsed with DOX for 2 min, thoroughly washed and a portion of the supernant was harvested after 2 h of incubation in fresh medium. The supernatants were diluted with medium at a ratio of 1:2, 1:4 and 1:8. The results are shown in Fig. 5 and as spheroid growth after a 14 day period in culture. In the absence of light treatment, the drug containing supernantants were inhibitory for spheroid growth only at the highest supernatant concentration (1:2 dilution). In contrast, spheroid growth inhibition was significantly enhanced by PCI, at both fluence levels tested, for all 3 dilutions. At the lowest light fluence (0.96 J/cm^2) calculated α − values were: 3.1 and 2.0 for dilutions of 1:2 and 1:8 respectively. This clearly indicates a synergistic response compared to drug or PDT applied separately as was also the case for PCI of free DOX (Fig. 4). In Fig. 3b, a DOX concentration of 0.1 μg/ml resulted in a spheroid volume of approximately 60% of control values by day 14. A 1:2 dilution of the DOX concentration in the supernatant resulted in a similar growth inhibition (Fig. 5, no PCI) indicating a DOX concentration of approximatly 0.2 μg/ml. Supernatants harvested from monolayers of empty Ma or from DOX loaded Ma monolayers 5 min following the wash procedure showed no inhibitory effects either with or without PCI (data not shown). This would indicate that the DOX in the supernatant was released from the Ma and was not simply due to drug remnants as a result of an insufficient Ma wash.

3.5. PCI effect on hybrid spheroid growth

The basic assumption for the use of Ma^{DOX} as delivery vehicles is that they will act as drug release centers throughout the tumor, and the released drug will be taken up by the tumor cell population. The number of Ma^{DOX} in proportion to the number of tumor cells in the tumor is therefore a critical factor. To simulate this situation in vitro, experiments were performed employing hybrid spheroids formed from F98 cells in combination with a variable subpopulation of Ma^{DOX} ranging from 11 to 33% of the initial total. The number of F98 cells was held constant (4×10^3) while the Ma^{DOX} were varied in order to obtain F98:Ma^{DOX} ratios of 8:1, 4:1 and 2:1. Control spheroids containing no Ma were also included. The growth of three hybrid spheroid groups were evaluated: a) F98/empty Ma, b) F98/Ma^{DOX} and c) PCI-F98/Ma^{DOX}. Since the Ma were treated with the mitosis inhibiting agent, mitomycin C, they did not contribute to the spheroid growth. The growth kinetics of the hybrid spheroids for all three experimental groups are shown in Fig. 6Aa–c. Empty Ma appeared to introduce a growth delay with the average spheroid volume less than controls on day 7 but did not significantly alter the growth characteristics of the spheroids, even at the highest number of Ma present in the spheroids as measured on day 14 (Fig. 6Aa). The effects of incorporation of Ma^{DOX} in the spheroids are shown in Fig. 6Ab. A significant growth inhibition was observed at both day 7 and day 14 for all three of the Ma^{DOX} cell numbers tested. Nevertheless, the spheroids were still in a growth phase and eventually

reached control values when monitored for a longer interval. Comparable spheroid models have been employed in several of our previous studies examining the effects of photodynamic and photothermal therapies on spheroid growth [8,19]. Regardless of treatment modality, insufficient doses often result in growth delay rather than growth cessation as demonstrated in Fig. 6Aa and Ab. In general, most of the proliferating cells in spheroids are found in the outer three to five cell layers (ca. 75 μm) and it is from these oxygen rich layers that spheroid growth is observed. Both drug and PDT exert their greatest effect on these outer cell layers. In contrast, quiescent cells located towards the spheroid center, i.e., in an oxygen poor environment, demonstrate greater resistance to treatment but can be recruited back into the cycling population as the cells in the outer layers are killed. Thus, after a delay, the spheroids renew their growth giving rise to the characteristic growth delay curves often observed. In contrast, PCI treatment of F98/Ma^{DOX} hybrid spheroids resulted in almost complete growth cessation as seen in Fig. 6Ac. Spheroid volumes were not significantly different on day 14 compared to day 3 ($p > 0.1$) for all three of the cell ratios examined. The corresponding α − values derived from the day 14 data shown in Fig. 6Ac ranged from 4 to 6 which is indicative of significant synergistic responses for the three cell ratios employed. Light micrograph images of typical hybrid spheroids following two weeks of growth show the synergistic effect of PCI treatment on the F98/Ma^{DOX} hybrid spheroids (Fig. 6B).

A similar hybrid spheroid model was used by Baek et al., consisting of human glioma cells and mouse macrophages loaded with gold nanoshells [8]. When these hybrid spheroids were exposed to near infrared light in photothermal therapy (PTT) experiments, significant spheroid growth inhibition via hyperthermia was achieved albeit at relatively high irradiances (14–28 W/cm^2). The irradiation time (10 min) was the same as that used in the PCI experiments presented here. Compared to the high laser irradiance required for effective PTT in the above described in vitro model, the irradiance needed (2 mW/cm^2) to induce the PCI effects observed in the present studies was orders of magnitude lower, thus demonstrating the high efficiency of the PCI Ma^{DOX} combination.

4. Conclusion

The experiments reported here investigated the utility of loaded macrophages, acting as drug transport vehicles, together with the light-based drug delivery technique PCI. The studies demonstrated that RAW264.7 Ma, pulsed with DOX, were capable of rapid release of the drug. Furthermore, PCI was found to increase the ability of free or Ma released DOX to inhibit the growth of tumor spheroids in vitro. The growth of F98 + Ma^{DOX} hybrid spheroids were synergistically reduced or completely inhibited by PCI compared to either PDT or Ma^{DOX} acting as single treatments.

Acknowledgments

Funding

This work was supported by the Norwegian Radium Hospital Research Foundation. [Grant nr 1503].

The authors are grateful for the support from the Norwegian Radium Hospital Research Foundation. Portions of this work were made possible through access to the LAMMP Program NIBIB P41EB015890 at UCI. Steen Madsen was supported, in part, by the Tony and Renee Marlon Charitable Foundation.

References

1. Fischbach MA, Bluestone JA, Lim WA. Cell-based therapeutics: the next pillar of medicine. Sci. Transl. Med. 2013; 5(179) http://dx.doi.org/10.1126/scitranslmed.3005568 (179ps7).
2. Basel MT, Shrestha TB, Bossmann SH, Troyer DL. Cells as delivery vehicles for cancer therapeutics. Ther. Deliv. 2014; 5(5):555–567. http://dx.doi.org/10.4155/tde.14.24. [PubMed: 24998274]
3. Mantovani A, Sica A, Sozzani S, Allavena P, Vecchi A, Locati M. The chemokine system in diverse forms of macrophage activation and polarization. Trends Immunol. 2004; 25(12):677–686. http://dx.doi.org/10.1016/j.it.2004.09.015. [PubMed: 15530839]
4. Raman D, Baugher PJ, Thu YM, Richmond A. Role of chemokines in tumor growth. Cancer Lett. 2007; 256(2):137–165. http://dx.doi.org/10.1016/j.canlet.2007.05.013. [PubMed: 17629396]
5. Martinez FO, Sica A, Mantovani A, Locati M. Macrophage activation and polarization. Front. Biosci. 2008; 13:453–461. [PubMed: 17981560]
6. Dreaden EC, Mwakwari SC, Austin LA, Kieffer MJ, Oyelere AK, El-Sayed MA. Small molecule–gold nanorod conjugates selectively target and induce macrophage cytotoxicity towards breast cancer cells. Small. 2012; 8(18):2819–2822. http://dx.doi.org/10.1002/smll.201200333. [PubMed: 22777707]
7. Muthana M, Giannoudis A, Scott SD, Fang HY, Coffelt SB, Morrow FJ, Murdoch C, Burton J, Cross N, Burke B, Mistry R. Use of macrophages to target therapeutic adenovirus to human prostate tumors. Cancer Res. 2011; 71(5):1805–1815. http://dx.doi.org/10.1158/0008-5472.CAN-10-2349. [PubMed: 21233334]
8. Baek SK, Makkouk AR, Krasieva T, Sun CH, Madsen SJ, Hirschberg H. Photothermal treatment of glioma; an in vitro study of macrophage-mediated delivery of gold nanoshells. J. Neurooncol. 2011; 104(2):439–448. http://dx.doi.org/10.1007/s11060-010-0511-3. [PubMed: 21221712]
9. Choi MR, Bardhan R, Stanton-Maxey KJ, Badve S, Nakshatri H, Stantz KM, Cao N, Halas NJ, Clare SE. Delivery of nanoparticles to brain metastases of breast cancer using a cellular Trojan horse. Cancer Nanotechnol. 2012; 3(1–6):47–54. http://dx.doi.org/10.1007/s12645-012-0029-9. [PubMed: 23205151]
10. Madsen SJ, Baek SK, Makkouk AR, Krasieva T, Hirschberg H. Macrophages as cell-based delivery systems for nanoshells in photothermal therapy. Ann. Biomed. Eng. 2012; 40(2):507–515. http://dx.doi.org/10.1007/s10439-011-0415-1. [PubMed: 21979168]
11. Fu J, Wang D, Mei D, Zhang H, Wang Z, He B, Dai W, Zhang H, Wang X, Zhang Q. Macrophage mediated biomimetic delivery system for the treatment of lung metastasis of breast cancer. J. Control. Release. 2015; 204:9–11. http://dx.doi.org/10.1016/j.jconrel.2015.01.039.
12. Li S, Feng S, Ding L, Liu Y, Zhu Q, Qian Z, Gu Y. Nanomedicine engulfed by macrophages for targeted tumor therapy. Int J Nanomedicine. 2016; 11:4107–4124. http://dx.doi.org/10.2147/IJN.S110146. [PubMed: 27601898]
13. Berg K, Folini M, Prasmickaite L, Selbo PK, Bonsted A, Engesaeter BO, Zaffaroni N, Weyergang A, Dietzea A, Maelandsmo GM, Wagner E. Photochemical internalization: a new tool for drug delivery. Curr. Pharm. Biotech. 2007; 8(6):362–372.
14. Selbo PK, Weyergang A, Høgset A, Norum OJ, Berstad MB, Vikdal M, Berg K. Photochemical internalization provides time-and space-controlled endolysosomal escape of therapeutic molecules. J. Control. Release. 2010; 148(1):2–12. http://dx.doi.org/10.1016/j.jconrel.2010.06.008. [PubMed: 20600406]
15. Mathews MS, Blickenstaff JW, Shih EC, Zamora G, Vo V, Sun CH, Hirschberg H, Madsen SJ. Photochemical internalization of bleomycin for glioma treatment. J. Biomed. Opt. 2012; 17(5) http://dx.doi.org/10.1117/1.JBO.17.5.058001 (0580011-8).
16. Weyergang A, Berstad ME, Bull-Hansen B, Olsen CE, Selbo PK, Berg K. Photochemical activation of drugs for the treatment of therapy-resistant cancers. Photochem. Photobiol. Sci. 2015; 14(8):1465–1475. http://dx.doi.org/10.1039/c5pp00029g. [PubMed: 25849953]

17. Lou PJ, Lai PS, Shieh MJ, MacRobert AJ, Berg K, Bown SG. Reversal of doxorubicin resistance in breast cancer cells by photochemical internalization. Int. J. Cancer. 2006; 119(11):2692–2698. http://dx.doi.org/10.1002/ijc.22098. [PubMed: 16991130]

18. Lai PS, Lou PJ, Peng CL, Pai CL, Yen WN, Huang MY, Young TH, Shieh MJ. Doxorubicin delivery by polyamidoamine dendrimer conjugation and photochemical internalization for cancer therapy. J. Control. Release. 2007; 122(1):39–46. http://dx.doi.org/10.1016/j.jconrel.2007.06.012. [PubMed: 17628166]

19. Madsen SJ, Sun CH, Tromberg BJ, Cristini V, De Magalhães N, Hirschberg H. Multicell tumor spheroids in photodynamic therapy. Lasers Surg. Med. 2006; 38(5):555–564. http://dx.doi.org/10.1002/lsm.20350. [PubMed: 16788918]

20. Canti G, Nicolin A, Cubeddu R, Taroni P, Bandieramonte G, Valentini G. Antitumor efficacy of the combination of photodynamic therapy and chemotherapy in murine tumors. Cancer Lett. 1998; 125(1):39–44. [PubMed: 9566694]

21. Mathews MS, Vo V, Shih EC, Zamora G, Sun CH, Madsen SJ, Hirschberg H. Photochemical internalization-mediated delivery of chemotherapeutic agents in human breast tumor cell lines. J. Environ. Pathol. Toxicol. Oncol. 2012; 31(1):49–59. [PubMed: 22591284]

22. Prasmickaite L, Høgset A, Selbo PK, Engesæter BØ, Hellum M, Berg K. Photochemical disruption of endocytic vesicles before delivery of drugs: a new strategy for cancer therapy. Br. J. Cancer. 2002; 86(4):652–657. http://dx.doi.org/10.1038/sj.bjc.6600138. [PubMed: 11870551]

23. Berstad MB, Weyergang A, Berg K. Photochemical internalization (PCI) of HER2-targeted toxins: synergy is dependent on the treatment sequence. Biochim. Biophys. Acta. 2012; 1820(12):1849–1858. http://dx.doi.org/10.1016/j.bbagen.2012.08.027. [PubMed: 22981913]

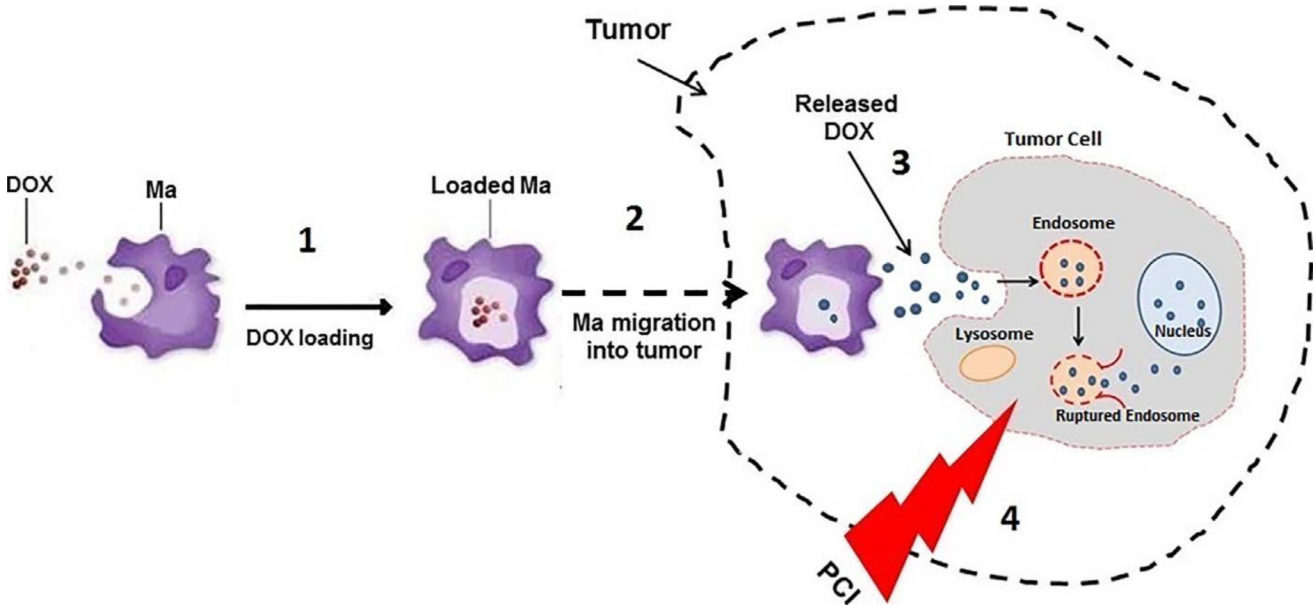

Fig 1.

Overview of PCI via Ma-mediated delivery of drug into tumors. (1) Ma incubated with DOX, forming loaded Ma. (2) Loaded Ma migrate to tumor cells incubated with photosensitizer, $AlPcS_{2a}$. (3) DOX, which is released with time, is incorporated into tumor cells by endocytosis. (4) Laser irradiation (PCI) leads to endosomal escape, significantly enhancing drug efficacy.

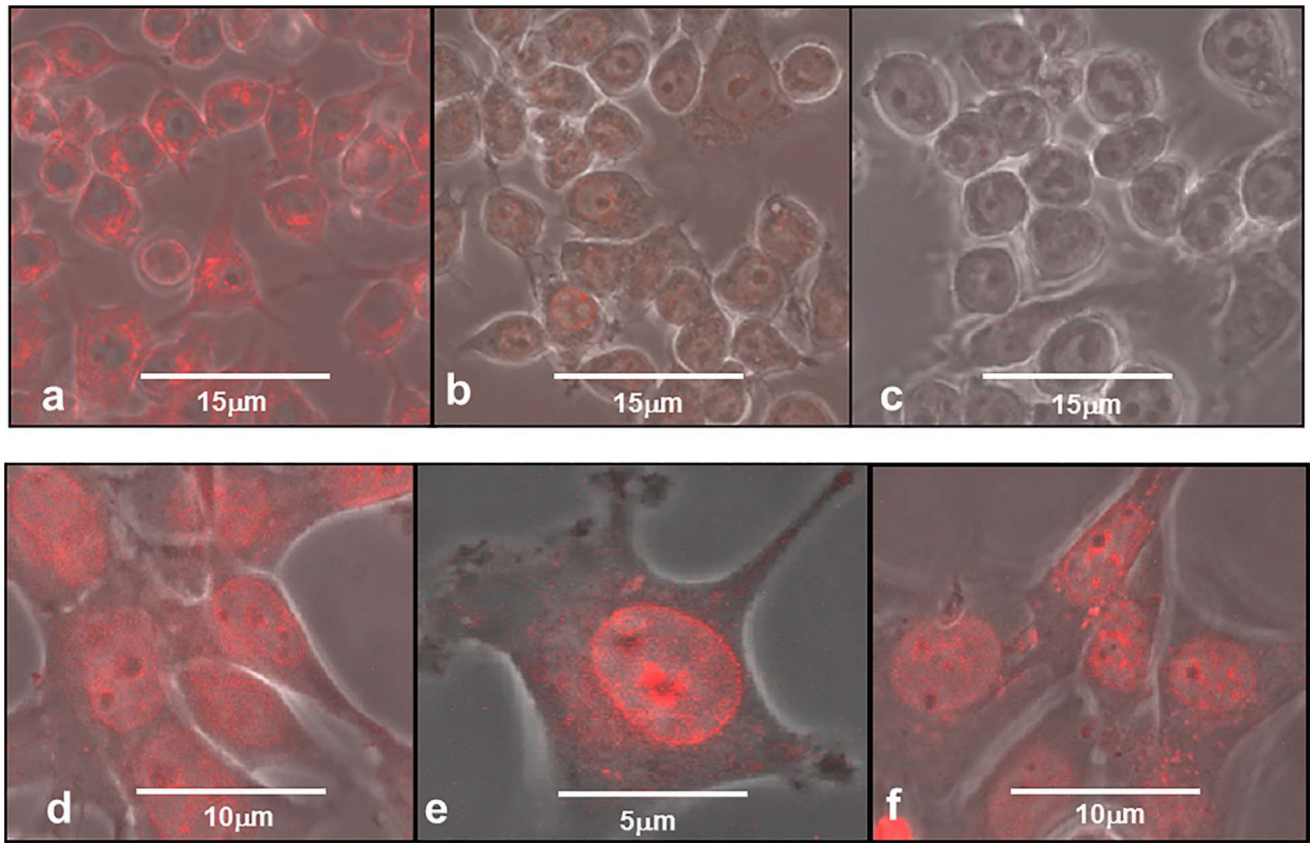

Fig. 2.

Confocal micrographs of drug release of DOX from Ma^{DOX} and F98. The cells were incubated with DOX: Ma 100 μg/ml for 2 min, F98 10 μg/ml for 30 min. DOX is shown by red fluorescence. (a) Ma^{DOX}, 15 min; (b) Ma^{DOX}, 120 min; (c) Ma^{DOX}, 180 min. (d) F98, 15 min; (e) F98, 15 min, with higher magnification (f) F98, 180 min. Scale bar as shown. (For interpretation of the references to colour in this figure legend, the reader is referred to the web version of this article.)

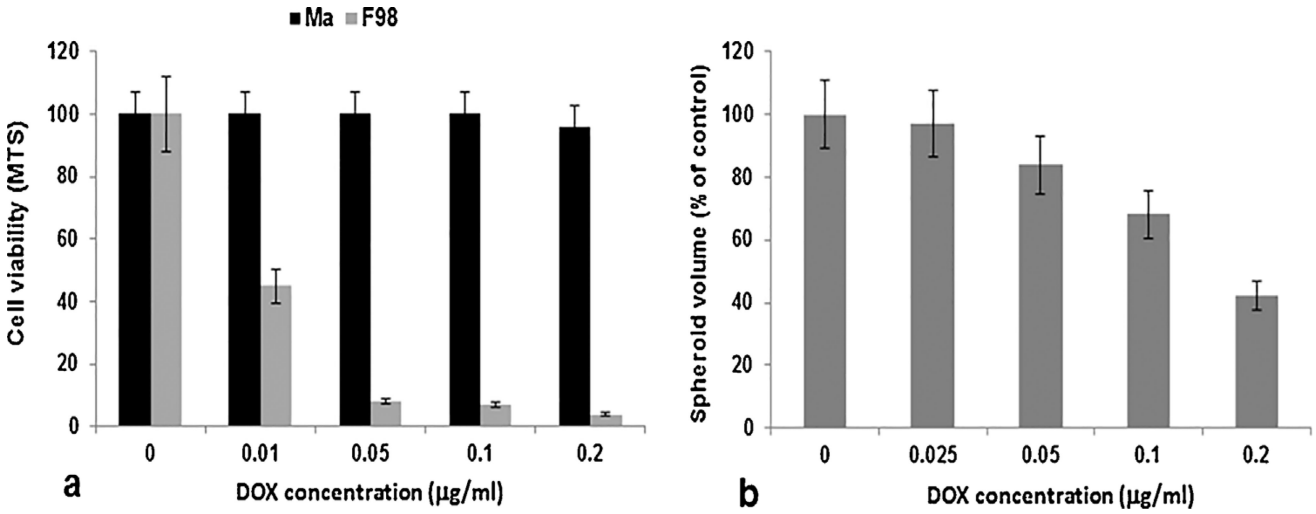

Fig. 3.

Toxic effect of DOX on Ma and F98 tumor cells. DOX was administered at varying concentrations (0–0.2 μg/ml). a) Effect of DOX on 5×10^3 cells of Ma or F98 tumor cells. Cell viability was assessed by MTS assay 96 h post drug administration. b) Effect of DOX on F98 spheroid growth over a 14 day incubation period. Each data point represents mean ± standard deviation of four trials.

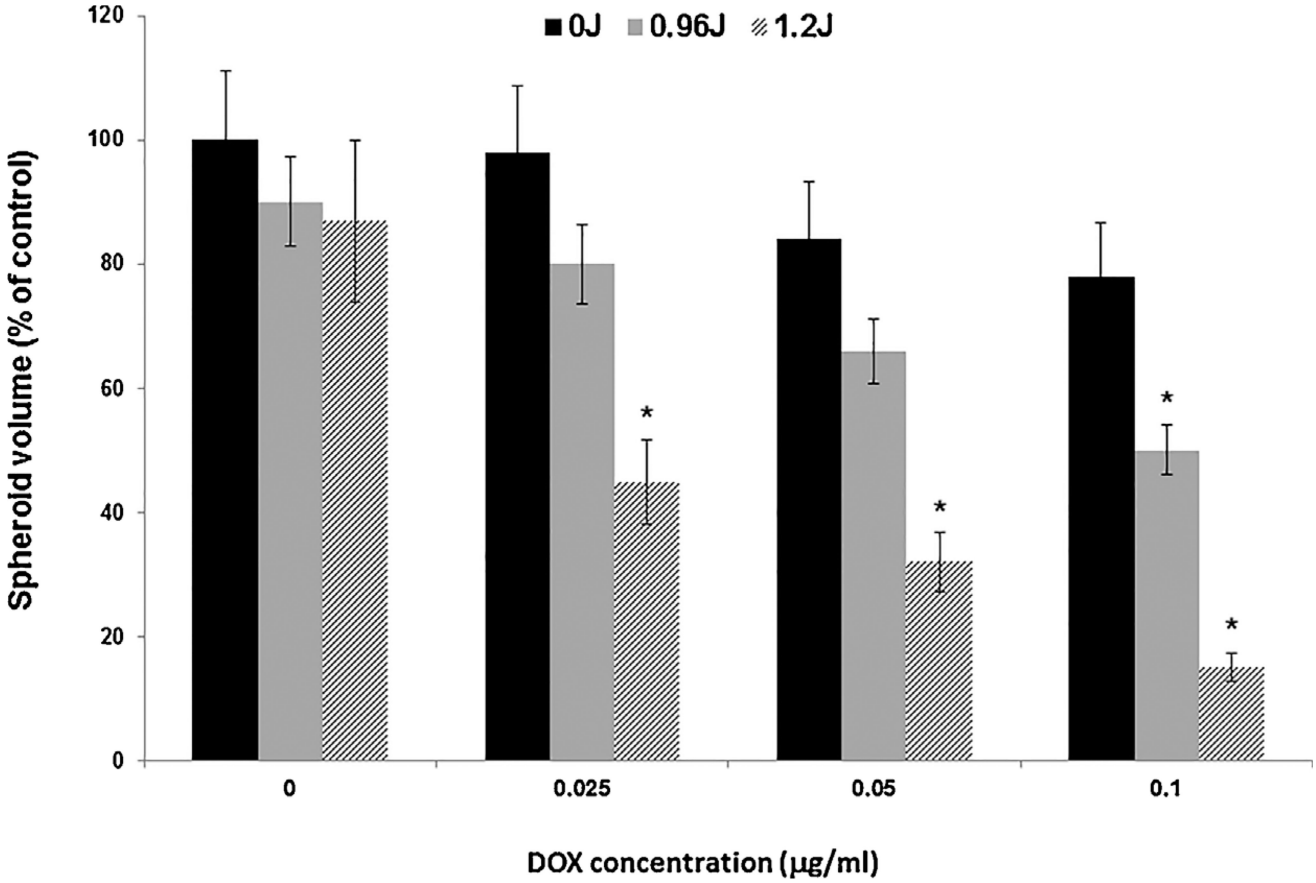

Fig. 4.

Effect of PCI on the growth of F98 spheroids treated with free DOX (0–0.1 μg/ml) and PCI at light fluence levels of 0, 0.96, and 1.2 J/cm^2. Each data point represents mean volume of 8 spheroids after 2 weeks in culture as a% of non-treated controls. Error bars denote standard deviations and * represents significant differences ($p < 0.05$) compared to controls.

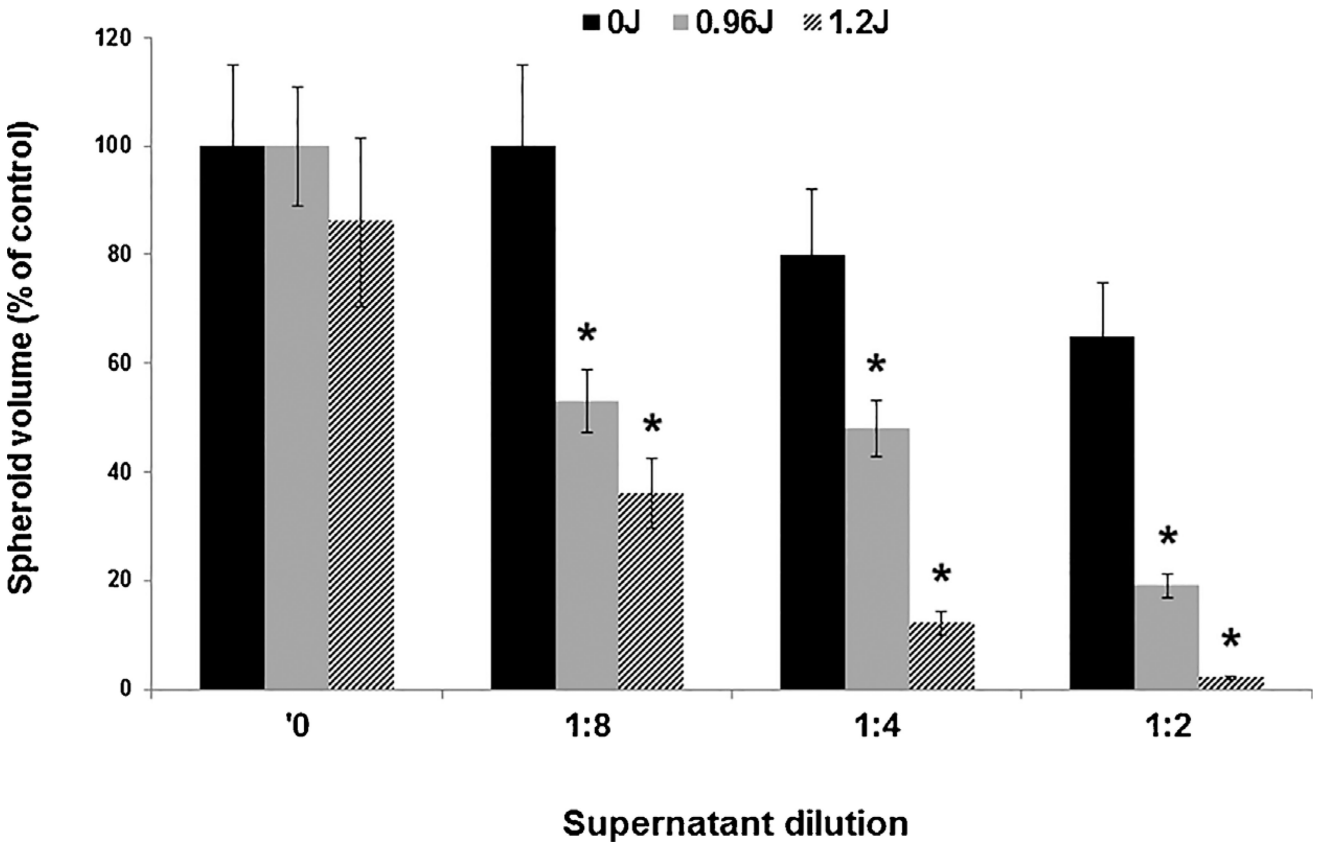

Fig. 5.

Effect of PCI on F98 spheroids incubated with supernatants released from DOX-loaded Ma. Ma were incubated with DOX for 2 min, washed, and given fresh medium. Supernatant/fresh medium ratios of 1:2, 1:4, and 1:8 were made and added to the F98 spheroids. PCI was performed using light fluence levels of 0, 0.96, and 1.2 J/cm^2. Each data point represents the mean volume of 16 spheroids from two experiments after two weeks in culture as a% of non-treated controls. Error bars denote standard deviations and * represents significant differences ($p < 0.05$) compared to controls.

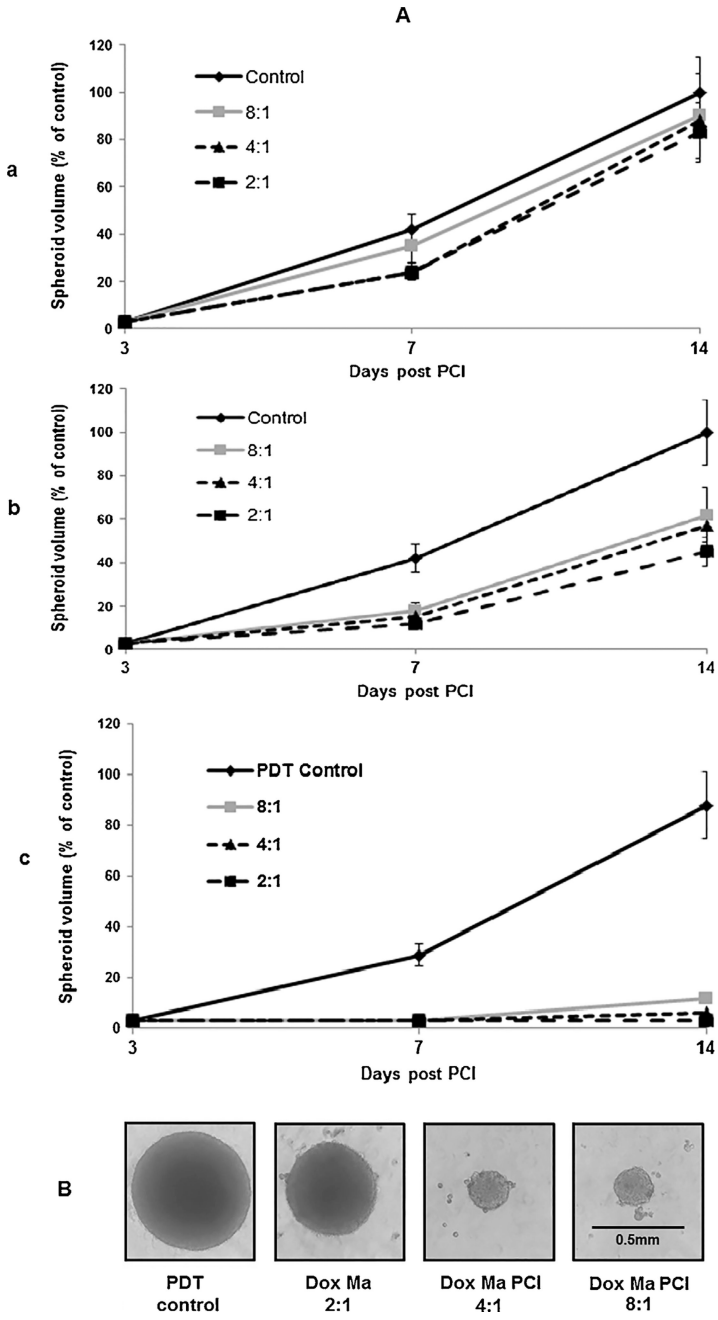

Fig. 6.

Effect of PCI on F98/Ma^{DOX} hybrid spheroids. Hybrid spheroids were formed with 4×10^3 F98 cells combined with varying numbers of either empty Ma or Ma^{DOX}. Ratios of F98/Ma used were 2:1, 4:1, and 8:1. (B) Light micrograph images of typical hybrid spheroids following two weeks of growth. (A) Spheroid volume growth kinetics: a) Empty Ma, b) loaded Ma^{DOX}, c) PCI with loaded Ma^{DOX}. PCI; radiant exposure = 1.2 J/cm^2. Each data point represents the mean volume of 16 spheroids from two experiments after two weeks in culture as a% of non-treated controls. Error bars; standard deviation.